Status report of the SAXO+ opto-mechanical design concept

Eric Stadler, Emiliano Diolaiti, Laura Schreiber, Fausto Cortecchia, Matteo Lombini, Magali Loupias, Yves Magnard, Adriano de Rosa, Guiseppe Malaguti, Didier Maurel, et al.

AO4ELT Proceedings: Status report of the SAXO+ opto-mechanical design concept

Eric Stadler*[1a], Emiliano Diolaiti[b], Laura Schreiber[b, a], Fausto Cortecchia[b], Matteo Lombini[b], Magali Loupias[c], Yves Magnard[a], Adriano De Rosa[b], Giuseppe Malaguti[b], Didier Maurel[a], Gianluca Morgante[b], Patrick Rabou[a], Sylvain Rochat[a], Filomena Schiavone[b], Luca Terenzi[b], Fabrice Vidal[d], Florian Ferreira[d], Eric Gendron[d], Johan Mazoyer[d], Mamadou Ndiaye[g] , Maud Langlois[c], Michel Tallon[c], Sylvain Rousseau[g] , Raffaele Gratton[f], Julien Milli[a], David Mouillet[a] , Gael Chauvin[g] , François Wildi[h] , Anthony Boccaletti[d]

[a]Univ. Grenoble Alpes, CNRS, IPAG, 38000 Grenoble, France;

[b]INAF - Osservatorio di Astrofisica e Scienza dello Spazio (OAS), Via Gobetti 93/3, Bologna, 40129, Italy;

[c]Univ Lyon, Univ Lyon1, Ens de Lyon, CNRS, Centre de Recherche Astrophysique de Lyon UMR5574, Saint Genis-Laval, F-69230, France;

[d]CNRS-LESIA UMR-8109 Observatoire de Paris, Section de Meudon 5, place Jules Janssen 92195 MEUDON Cedex, France;

[e]Aix Marseille Univ., CNRS, CNES LAM, 38 rue F. Joliot-Curie, 13388, Marseille, France;

[f]INAF - Osservatorio Astronomico di Padova, Vicolo dell'Osservatorio 5, Padova, 35122, Italy;

[g]Lagrange Laboratory Côte d'Azur Observatory, UMR 7293 Bâtiment H. Fizeau, 28, Avenue Valrose Nice cedex 2, 06108, France;

[h]Univeristy of Geneva, Dept of Astronomy, Ch. Pegasi 51, CH-1290 Sauverny, Switzerland

ABSTRACT

SAXO+ is the second-stage adaptive optics module for the SPHERE instrument at VLT, proposed to boost the current performances of detection and characterization of exoplanets and as a pathfinder for the future planet finder (PCS) of the European ELT. It will work in combination with the SAXO first-stage xAO system measuring and reducing the residual wavefront errors. SAXO+ will be implemented on a mezzanine above the main bench and it will be fed by an exchange mechanism deploying a pick-off mirror in order to preserve all the functionalities of the original instrument. Optical interfaces at the output are left unchanged for the scientific instruments downstream. We present in this paper the current status of the SAXO+ baseline opto-mechanical design and its major challenges.

Keywords: Extreme Adaptive Optics, Optical Design, Mechanical Design, SPHERE, VLT, ELT, instrument upgrades, SAXO+

1. INTRODUCTION

SPHERE+[1] is a proposed upgrade of the SPHERE[2] instrument at VLT, which will boost the current performances of detection and characterization of exoplanets and disks, and will serve as a demonstrator for the future planet finder (PCS[3]) of the European ELT[4]. The upgrade aims at improving the raw contrast (up to 10^{-5}, goal 10^{-6}) close to the optical axis (at separation of 0.2 as, goal 0.1 as), enabling the observation of fainter and redder targets. The contrast gain will be made possible by a second-stage Adaptive Optics (AO) module (hereafter SAXO+[1]) combined with the currently operating first-stage extreme Adaptive Optics (xAO) system (SAXO[5]). SAXO+ will offer moderate spatial sampling (in the order of 20-30 actuators across the pupil) and fast correction frame rate (up to 3 kHz); it will measure

*eric.stadler@univ-grenoble-alpes.fr

and reduce wavefront errors left by SAXO. This paper is focused on the optical and mechanical implementation of SAXO+ within SPHERE[6]. In order to preserve the current functionalities, the second-stage opto-mechanical module is designed as a sort of switchable optical by-pass. It is compact, due to space constraints, and offers good accessibility for installation and maintenance. Optical interfaces at the output are left unchanged for the scientific instruments downstream. The module offers two internal pupil images for the second-stage adaptive deformable mirror and a deployable apodizer for coronographic observations. A dichroic beam-splitter feeds the second-stage pyramid-based infrared wavefront sensor. The paper gives an overview of the requirements and of the current baseline concept. A novel concept for the pyramid wavefront sensor (PyrWFS) dynamic modulation device, based on a rotary stage motor, is also presented.

2. REQUIREMENTS

The main requirements of the SAXO+ opto-mechanical module are summarized in Table 1.

Table 1. Main requirements.

Requirement	**Value**
Common path	
Operational	It shall be possible to optically by-pass SAXO+ by a deployable mechanism
Dimensional	Maximum available space in plant ~ 1200 mm × 600 mm Maximum height above SPHERE bench ~ 950 mm Main optical axis of SAXO+ shall be 400 mm above SPHERE optical axis SAXO+ light pick-off between the SPHERE Atmospheric Dispersion Compensator and Differential Tip-Tilt Sensor beam-splitter
Optical interfaces	Same as SPHERE without SAXO+
Wavelength range	0.95 – 2.32 µm
Field of view	17.3 arcsec diameter
Pupil planes inside SAXO+	two pupil planes required (deformable mirror, deployable apodiser)
Diameter of pupil image for DM	~10 mm
Diameter of pupil image for apodiser	3 – 18 mm, for manufacturing reasons
Dichroic beam-splitter properties	Long-pass
Dichroic beam-splitter position	Close to intermediate focal plane, with accessible focal plane at WFS input
Polarisation effects	Polarisation vector direction to remain unchanged through SAXO+
Wavefront sensor path	
Wavefront sensor type	Pyramid
Wavelength range	0.95 – 1.1 µm, bright case 0.95 – 1.4 µm (possible extension to 1.8 µm), faint case
Field of view	3.2 arcsec diameter
Focal ratio on pyramid prism	F/20 – F/40
Tip-tilt modulation	Modulation radius up to 5 λ/D to be confirmed
Slow tip-tilt drift compensation	Required
Pupil registration on WFS detector	Required
Pupil image diameter on WFS detector	1.2 mm, corresponding to 50 pixels for 24 µm pixel pitch

The optical design optimization is also driven by general performance requirements (wavefront error on intermediate and output focal planes, pupil imaging quality on pupil planes) which are under consolidation at the moment of this writing in the framework of the system budgets definition.

3. PRELIMINARY DESIGN

3.1 Optical design

The baseline optical design is the outcome of a trade-off among five concepts, to explore different solutions regarding overall layout and volume, accessibility, position and configuration of specific components such as the dichroic beam-splitter. The design is shown in Figure 1.

The optical beam from the SPHERE optics is picked-off by a deployable fold mirror in order to feed SAXO+, and then re-injected into the SPHERE optical path by another deployable fold mirror. For opto-mechanical reasons, the two fold mirrors, and a lens to form the SAXO+ output focal plane, are mounted on the same deployment mechanism. When the deployable group is out of the optical beam, SAXO+ is simply skipped.

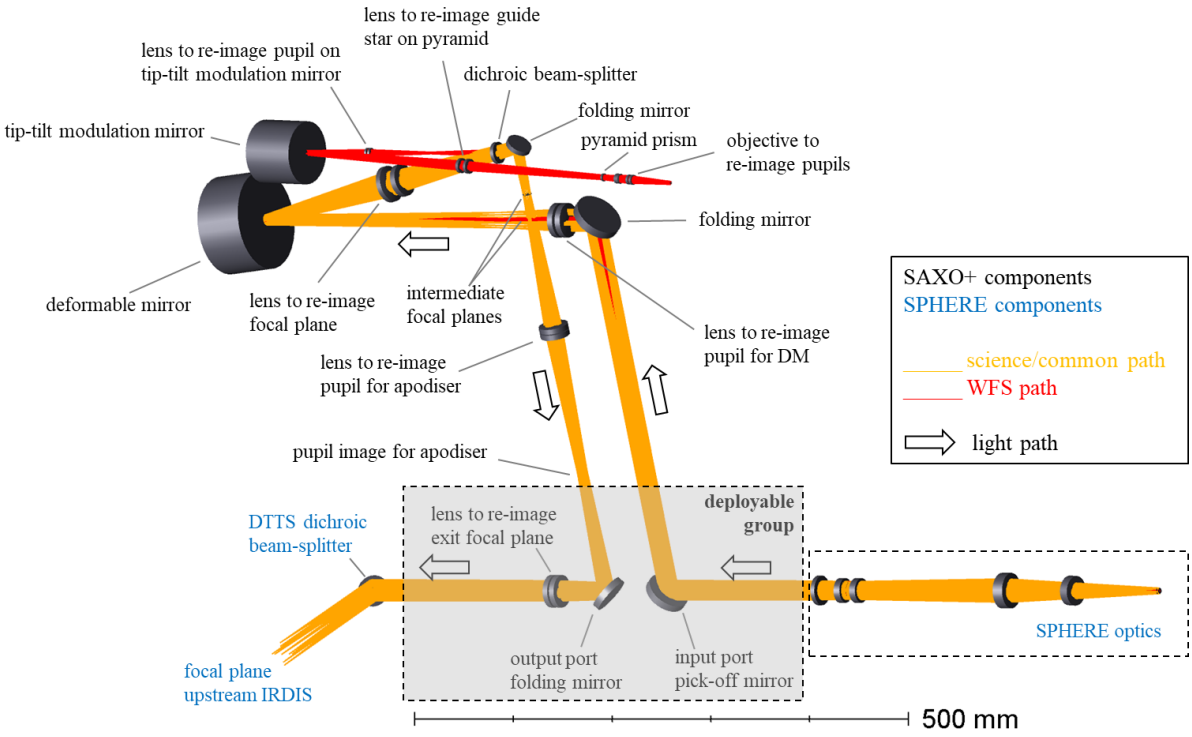

Figure 1. Second-stage AO module optical design.

The science/common path consists of four air-spaced doublet lenses. The first doublet lens forms a pupil image on the Deformable Mirror (DM); the pupil image diameter is about 10 mm and may be enlarged by about 30% by design re-optimisation without significant changes in the overall layout. The second doublet lens forms an intermediate focal plane where a dichroic beam-splitter splits the WFS path (in reflection) from the common path (in transmission); the beam-splitter is positioned in such a way to leave clearance around the reflected focal plane in the WFS path for positioning, if necessary, a deployable calibration source. The third doublet lens forms a pupil image for a deployable apodiser. Finally, the fourth doublet lens (mounted on the deployable pick-off group described above) forms the output focal plane. The optical beam in the common path is folded by five mirrors, one of which is the DM. Some, or all, the remaining four fold mirrors could be used for optical beam alignment and two of them also serve the function to pick-off the light beam for SAXO+ and inject it back into the SPHERE main path, as already explained.

The WFS path consists of an air-spaced doublet lens which forms a 5 mm diameter pupil image on the tip-tilt modulation mirror, an air-spaced doublet lens which forms a telecentric F/40 focal plane on the pyramid prism and a three-lens pupil imaging objective to form four pupil images on the WFS camera with appropriate back-focal length.

Given the broad wavelength range of the WFS path, a simple pyramid prism made of infrared-transmitting material produces significant chromatic blur on the four pupil images. A double achromatic pyramid design has been therefore implemented: the choice of the two materials is under optimization at the moment of this writing, but a preliminary design indicates that chromatic effects can be reduced to negligible level, while assuring very high transmission over the whole wavelength range.

The optical performance of the current SAXO+ optical design is excellent. The nominal polychromatic Strehl Ratio is of the order of 99% at all intermediate and output focal planes, both in the common path and in the WFS path. The optical quality of the pupil images is well within the requirement of 1/10 of the relevant pitch/subaperture size. An error budget is under development, to account for manufacturing and alignment tolerances and for dynamic effects such as thermo-elastic variations depending on temperature changes.

3.2 Mechanical design

The preliminary mechanical design does not show obvious showstoppers. The main components are located on a platform situated over the SPHERE optical path (see Figure 2). Since it is not possible to drill new holes on the SPHERE bench, the main challenge is represented by the fact that this structure must be stiff enough while having only two legs. The structure will be optimised by Finite Element Analysis (FEA) to reach the best stiffness/mass ratio and it will be made of aluminum 5083 as the SPHERE bench to avoid any thermal differential effect.

The mechanical design will be finalised after definition of baseline optical design with trade off on DM specifications. All adjustments and the related ranges will be defined by the optical tolerance analysis. After this step, the mechanical design, with appropriate solutions for each movement, will be completed.

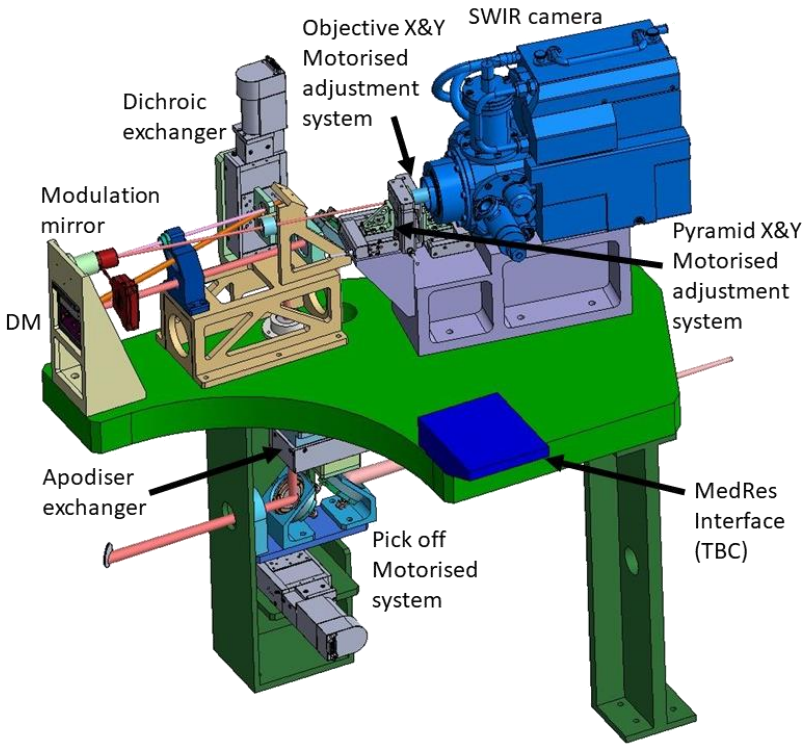

Figure 2. Preliminary mechanical design.

4. WAVEFRONT MODULATION

Most of xAO systems are using today Pyramid Wave Front Sensing[8] (PyrWFS). The PyWFS is one of the most sensitive WFSs, but it quickly saturates its linear regime. Modulating the wavefront in tip-tilt distributes the source light on all the faces of the pyramid, allowing linear measurements of the wavefront slope.

Current existing systems based on PyrWFS rely on fast piezo-electric off-the-shelf tip-tilt systems actuating a mirror to reach working frequencies up to about 1 kHz. Some laboratory tests have been done up to 3 kHz with components which were not adapted for such a high speed.

We will test existing components with improved controller to increase the speed, and we propose two promising alternative developments: a static optical approach[9][10][11] and a rotary prototype[6].

The current optical design of the SAXO+ WFS path is shown in the next figure: it is based on the assumption that tip-tilt modulation is performed by a reflective device in a pupil plane. The pupil image diameter is d = 5 mm. For the maximum required modulation radius (5 λ/d) at the longest wavefront sensing wavelength (λ = 1.8 μm), the optical deflection of the beam is 1.8 mrad, which is within the capabilities of existing commercial devices, at least in terms of amplitude. Smaller optical deflection angle may be achieved by increasing the diameter of the pupil image, at the expense of a larger size and mass of the mirror, which in general terms makes it more difficult to reach high modulation frequencies. Moreover, increasing the pupil image diameter impacts the WFS layout, which is constrained by tight volume allocation requirements.

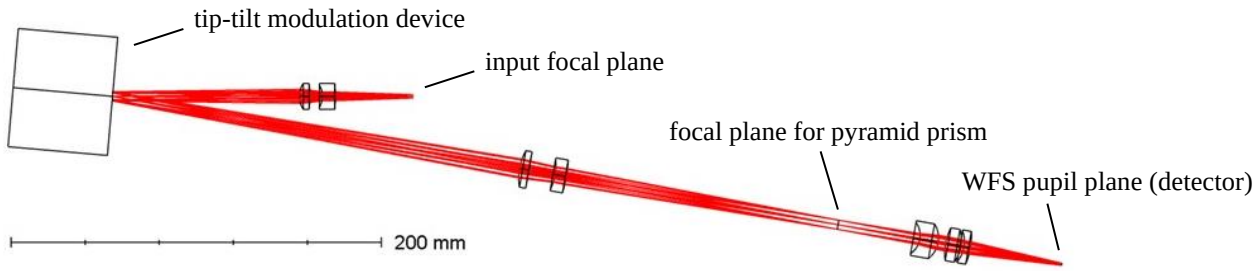

Figure 3. Pyramid Wave Front Sensor optical path (the double pyramid prism is not shown).

4.1 Tip-Tilt mirror approach

A tip-tilt mirror represents the classical approach. It works properly when the modulation is relatively slow and can be realized with standard components working at frequencies up to 1kHz in closed loop control with a long lifetime. The choice of this kind of device relies on the demonstration that it is possible to work at higher frequencies, up to 3kHz, maintaining an acceptable lifetime.

We are also looking for possible customised or modified products with manufacturers to reach our specifications.

4.2 Static modulation options

The use of static modulation overcomes the issues of spreading or shaping the PSF on the desired pyramid area without the need of dynamic components working at high speed. This makes this approach of easier implementation and maintenance. On the other hand, this approach is not implemented in any existing system up to now and would require in-depth investigation and testing.

We plan to study and test different static modulation patterns (Figure 4) and different technologies:

- Multiple-beam 2D patterns: this could be implemented by using a 2D holographic beam-splitter to split a single laser beam into several beams each with the characteristics of the original one. Another interesting approach would be implementing the Crossed-Cube double beam-splitter used for nulling interferometry[12];
- Circular patterns (with or without central light concentration): this shape could be realised by a Diffractive Optical Element (DOE) ring generator;
- Extended diffused light (e.g. Gaussian distribution): this solution represents a more classical diffuser pattern and could be realised by different techniques like phase grating, sand-blasted diffusers (in reflection or in transmission), holographic diffusers of liquid crystals.

Some important issues to be investigated are the transmissivity, the wavefront error introduced by this kind of element and the chromatism.

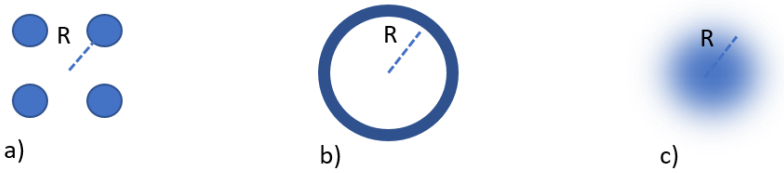

Figure 4. Different PSF shaping proposed for PyrWFS static modulation. R is the modulation radius. a) 2D holographic beam-splitter; b) DOE Ring generator (axicone); c) Diffused gaussian profile.

4.3 Rotary stage option

Two prototypes of rotary tip-tilt stage have been implemented.

The first prototype (Figure 5) was based on an additive manufacturing mirror holder part. This choice turned out to be too small for this manufacturing process, bringing to low precision and to important unbalance. For these reasons, during the first high speed test the shaft broke before 180 000 rpm. An analysis done with a microscope showed that the diameter of the flexible shaft was not regular.

Other issues might be due to the material characteristics with the additive manufacturing process. The geometric dimensions were in fact at the limits of this manufacturing technology.

Some improvements have been done on the second prototype design (Figure 6) to increase overall performances:

- Mirror holder manufacturing precision;
- Magnets manufactured to increase magnetic density;
- 3 parts coil holder to maximize the magnetic field;
- Optical baffle included.

The geometry of the mirror holding part has been redesigned to be machined with traditional equipment in aeronautical grade materials to obtain the optimal mechanical performances. Magnets have been designed and manufactured to maximise magnetic density (compared to standard commercial products). The coil has been calculated more precisely and a complete magnetic field analysis has been performed to design a ferromagnetic encapsulation made of three steel parts (in green and yellow on the picture below). The goal of these improvements was to increase the stiffness of the flexible shaft and obtain a first eigenfrequency of the system over 3 kHz.

The ultra-high speed motor used for the two first prototypes is based on classical ball bearing. This solution presents some major disadvantages: the bearing lifetime is estimated around 1000 hours and some vibrations appear at different ranges of frequencies.

For the next prototypes we are looking for electric motors with air bearing to solve these two major problems.

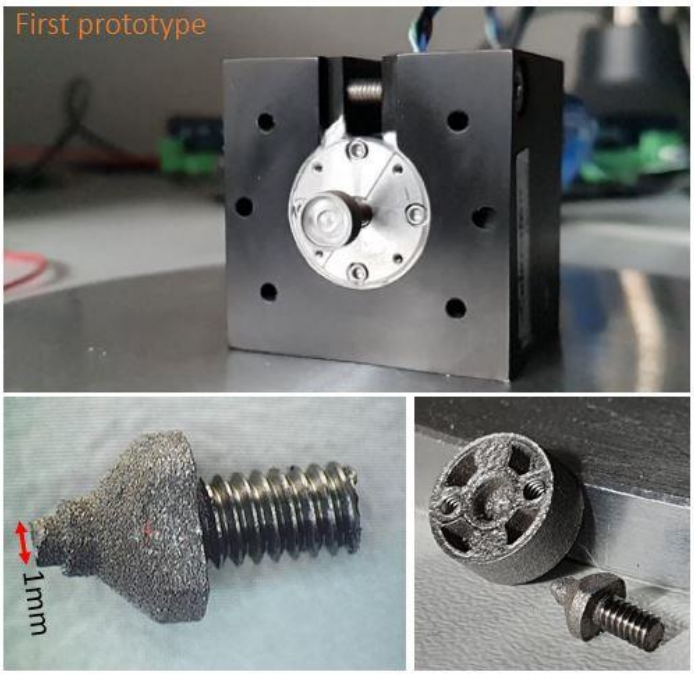

Figure 5. First rotary modulation prototype test.

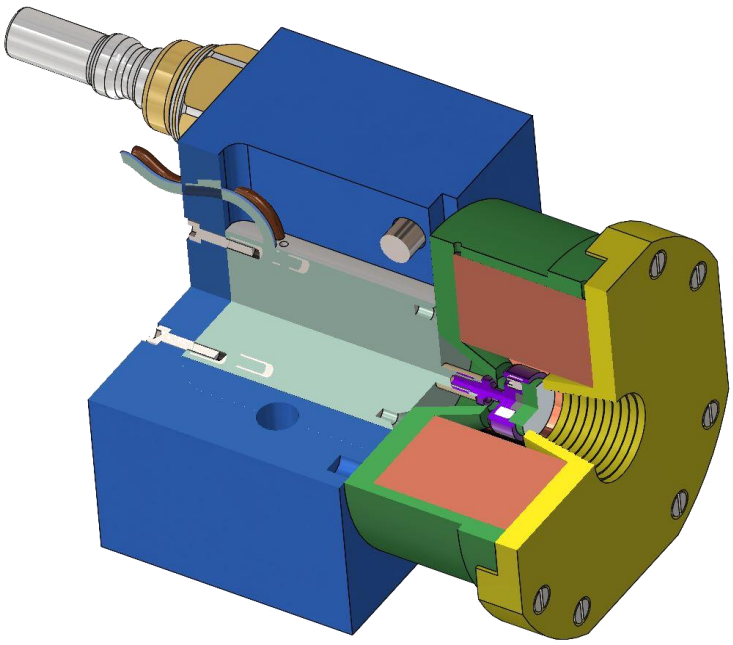

Figure 6. Design of second model of rotary prototype.

REFERENCES

[1] A. Boccaletti, G. Chauvin, F. Wildi, J. Milli, E. Stadler, E. Diolaiti, R. Gratton, F. Vidal, M. Loupias, M. Langlois, F. Cantalloube, M. N'Diaye, D. Gratadour, F. Ferreira, M. Tallon, J. Mazoyer, D. Segransan, D. Mouillet, J.-L. Beuzit, M. Bonnefoy, R. Galicher, A. Vigan, I. Snellen, M. Feldt, S. Desidera, S. Rousseau, A. Baruffolo, C. Goulas, P. Baudoz, C. Bechet, M. Benisty, A. Bianco, B. Carry, E. Cascone, B. Charnay, E. Choquet, V. Christiaens, F. Cortecchia, V. Di Capprio, A. De Rosa, C. Desgrange, V. D'Orazi, S. Douté, M. Frangiamore, E. Gendron, C. Ginski, E. Huby, C. Keller, C. Kulcsár, R. Landman, S. Lagarde, E. Lagadec, A.-M. Lagrange, M. Lombini, M. Kasper, F. Ménard, Y. Magnard, G. Malaguti, D. Maurel, D. Mesa, G. Morgante, E. Pantin, T. Pichon, A. Potier, P. Rabou, S. Rochat, l. Terenzi, E. Thiébaut, I. Tallon-Bosc, H.-F Raynaud, D. Rouan, A. Sevin, F. Schiavone, L. Schrieber, and A. Zanutta "Upgrading the high contrast imaging facility SPHERE: science drivers and instrument choices", Proc. SPIE 12184, Ground-based and Airborne Instrumentation for Astronomy IX, 121841S (2022)

[2] Beuzit, J. L., Vigan, A., Mouillet, D., Dohlen, K., Gratton, R., Boccaletti, A., Sauvage, J. F., Schmid, H. M., Langlois, M., Petit, C., Baruffolo, A., Feldt, M., Milli, J., Wahhaj, Z., Abe, L., Anselmi, U., Antichi, J., Barette, R., Baudrand, J., Baudoz, P., Bazzon, A., Bernardi, P., Blanchard, P., Brast, R., Bruno, P., Buey, T., Carbillet, M., Carle, M., Cascone, E., Chapron, F., Charton, J., Chauvin, G., Claudi, R., Costille, A., De Caprio, V., de Boer, J., Delboulb´e, A., Desidera, S., Dominik, C., Downing, M., Dupuis, O., Fabron, C., Fantinel, D., Farisato, G., Feautrier, P., Fedrigo, E., Fusco, T., Gigan, P., Ginski, C., Girard, J., Giro, E., Gisler, D., Gluck, L., Gry, C., Henning, T., Hubin, N., Hugot, E., Incorvaia, S., Jaquet, M., Kasper, M., Lagadec, E., Lagrange, A. M., Le Coroller, H., Le Mignant, D., Le Ruyet, B., Lessio, G., Lizon, J. L., Llored, M., Lundin, L., Madec, F., Magnard, Y., Marteaud, M., Martinez, P., Maurel, D., M´enard, F., Mesa, D., M¨oller-Nilsson, O., Moulin, T., Moutou, C., Orign´e, A., Parisot, J., Pavlov, A., Perret, D., Pragt, J., Puget, P., Rabou, P., Ramos, J., Reess, J. M., Rigal, F., Rochat, S., Roelfsema, R., Rousset, G., Roux, A., Saisse, M., Salasnich, B., Santambrogio, E., Scuderi, S., Segransan, D., Sevin, A., Siebenmorgen, R., Soenke, C., Stadler, E., Suarez, M., Tiph`ene, D., Turatto, M., Udry, S., Vakili, F., Waters, L. B. F. M., Weber, L., Wildi, F., Zins, G., and Zurlo, A., "SPHERE: the exoplanet imager for the Very Large Telescope," Astron. & Astrophys. 631, A155 (Nov. 2019)

[3] Kasper, M., Cerpa Urra, N., Pathak, P., Bonse, M., Nousiainen, J., Engler, B., Heritier, C. T., Kammerer, J., Leveratto, S., Rajani, C., Bristow, P., Le Louarn, M., Madec, P.-Y., Ströbele, S., Verinaud, C., Glauser, A., Quanz, S. P., Helin, T., Keller, C., Snik, F., Boccaletti, A., Chauvin, G., Mouillet, D., Kulcsár, C., Raynaud, H. –F, "PCS — A Roadmap for Exoearth Imaging with the ELT," The Messenger, vol. 182, p. 38-43 (2021)

[4] Tamai, R., Koehler, B., Cirasuolo, M., Biancat-Marchet, F., Tuti, M., González-Herrera, J-C, "The ESO's ELT construction progress," Proceedings of the SPIE, Volume 11445, id. 114451E 16 pp. (2020)

[5] C. Petit, J.-F. Sauvage, T. Fusco, A. Sevin, M. Suarez, A. Costille, A. Vigan, C. Soenke, D. Perret, S. Rochat, A. Barrufolo, B. Salasnich, J.-L. Beuzit, K. Dohlen, D. Mouillet, P. Puget, F. Wildi, M. Kasper, J.-M. Conan, C. Kulcsár, and H.-F. Raynaud "SPHERE eXtreme AO control scheme: final performance assessment and on sky validation of the first auto-tuned LQG based operational system", Proc. SPIE 9148, Adaptive Optics Systems IV, 91480O (2014)

[6] E. Stadler, E. Diolaiti, L. Schreiber, F. Cortecchia, M. Lombini, M. Loupias, Y. Magnard, A. De Rosa, G. Malaguti, D. Maurel, G. Morgante, P. Rabou, S. Rochat, F. Schiavone, L. Terenzi, F. Vidal, F. Cantalloube, E. Gendron, R. Gratton, J. Milli, D. Mouillet, G. Chauvin, F. Wildi, J.-L. Beuzit, A. Boccaletti, "SAXO+, a second-stage adaptive optics for SPHERE on VLT: optical and mechanical design concept," Proc. SPIE 12185, Adaptive Optics Systems VIII, 121854E (2022)

[7] A. Tozzi, P. Stefanini, E. Pinna, and S. Esposito "The double pyramid wavefront sensor for LBT", Proc. SPIE 7015, Adaptive Optics Systems, 701558 (2008)

[8] Ragazzoni R., "Pupil plane wavefront sensing with an oscillating prism," Journal of Modern Optics vol. 43, Issue 2, p.289-293

[9] R.Ragazzoni, E. Diolaiti, E. Vernet, "A pyramid wavefront sensor with no dynamic modulation", Opt. Commun. 208 (1-3), 51-60 (2002)

[10] J. LeDue, L. Jolissaint, J.-P. Véran, C. Bradley, "Calibration and testing with real turbulence of a pyramid sensor employing static modulation," Opt. Express 17, 7186-7195 (2009)

[11] L. Marafatto, R. Ragazzoni, D. Vassallo, M. Bergomi, F. Biondi, J. Farinato, D. Greggio, D. Magrin, and V. Viotto "Revisiting static modulation in pyramid wavefront sensing", Proc. SPIE 9912, Advances in Optical and Mechanical Technologies for Telescopes and Instrumentation II, 99122Q (2016)
[12] F. Hénault, A. Spang, "Cheapest nuller in the world: crossed beamsplitter cubes", Proc. SPIE 9146, Optical and Infrared Interferometry IV, 914604 (2014)